Luedeke et al. http://www.jcb.org/cgi/doi/10.1083/jcb.200412143

In silico modeling

Computational modeling was performed with the following goals. First, experimental data indicate that exchange of ER membrane proteins between the mother cell and the bud is very slow compared with protein mobility within these two compartments. Thus, we asked whether this difference is solely due to geometrical constraints at the bud neck or to more specific diffusion limitations at the bud neck. For this study, the exchange between the mother cortical ER and the bud ER was compared with the exchanges observed between the mother cortex and the perinuclear ER. Morphologically (as judged by electron and fluorescence microscopy), none of the connections between mother and bud cortices and between the mother cortex and the nucleus appear to be more prominent. Furthermore, we observed that exchange through the bud neck was much more rapid for the luminal protein GFP-HDEL than for Sec61-GFP and Sec22-GFP. Therefore, we asked whether the differences observed between the ER membrane and ER luminal proteins are due to the fact that they move in two- and three-dimensional spaces, respectively, and have different molecular diffusion constants. Finally, our model helped to investigate whether exchanges between mother and bud could be dependent on vesicular transport.

Model description and parameter identification

Consistent with our sodium azide experiments (Fig. 4), preliminary calculations using simple (first order) models showed that all experimental data could be explained assuming passive diffusion as the mechanism of transport (not depicted). The differences in the decay rates of the nonbleached compartments between membrane and luminal markers (Figs. 1 and 3) could be due to the different molecular diffusion constants of the two protein species Sec61-GFP and GFP-HDEL. The molecular diffusion constant of GFP-HDEL is ~40 times larger than the one of Sec61-GFP (GFP-KDEL: 10–30 $\mu m^2/s$ [Dayel et al., 1999]; Sec61 typical value for membrane proteins: 0.5 $\mu m^2/s$ [Lippincott-Schwartz et al., 2001]). To investigate this, a time-resolved diffusion transport model of the system was developed in order to derive numerical quantities that allow comparison between different FLIP experiments, taking into account influences of dimensionality (two- vs. three-dimensional spaces) or differences in the diffusion constants between species. The model is formulated based on physical principles (conservation of mass and momentum). It contains parameters of unknown value that need to be identified from data by means of model fitting.

On the time scale of a FLIP experiment (a couple of minutes), the only relevant dynamic processes are mass exchange between the mother cortex and the bud, mass exchange between the perinuclear and the cortical ER of the mother cell, and fluorescence drain due to photobleaching. These processes were fully resolved in the model. Faster dynamics (e.g., individual bleach pulses, switching of the laser, and camera dynamics) were modeled using algebraic (static) equations and slow dynamics (e.g., changes in shape or size of cells and changes in temperature) were neglected. Spatial distributions of protein within the same ER compartment were not resolved because they level out on a much faster time scale than the FLIP cycles (Fig. S1 and Fig. 1 C). Compensation for spontaneous bleaching during imaging was not done in the model itself (as this would unnecessarily add another unknown model parameter), but by normalization of the fluorescence pixel intensities I in each FLIP image: $(I - I_g)/(I_c - I_g)$. I_g is the average intensity level in the image background and I_c is the average intensity at the same time in the same compartment of a control cell to which no FLIP bleaching was applied.

The system was abstracted as shown in Fig. S2 A. The three distinct ER compartments correspond to the perinuclear ER (yellow), the cortical ER of the mother cell (blue), and the cortical ER of the bud (pink). Each compartment contains a certain amount (mass) of fluorescent protein as a function of time ($n(t)$, $m(t)$, and $b(t)$) and has a certain volume (V_n, V_m, and V_b). The compartments are assumed to be connected by passive diffusion. This assumption is supported by our sodium azide experiment (Fig. 4). Each connection is characterized by its effective cross section area (perimeter

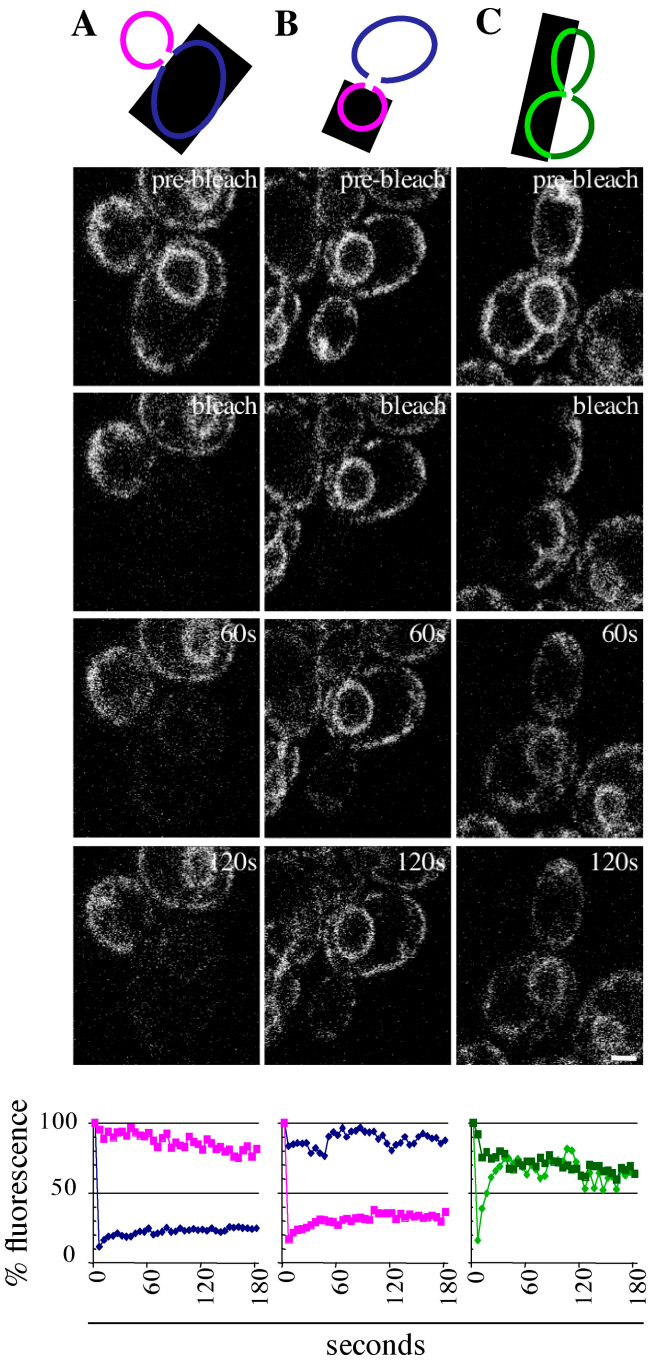

Figure S1. **FRAP analysis of Sec61-GFP through the bud neck.** (A) Bleaching the mother cortex, as depicted in the cartoon as in Fig. 2. Pictures of relevant time points. Graph shows kinetics of fluorescence recovery. $t_{1/2}$ of bleached compartment = 163 ± 93, n = 5. (B) Bleaching the bud cortex. Same color code as in Fig. 2. $t_{1/2}$ of bleached compartment = 118 ± 27, n = 5. (C) Bleaching along a longitudinal axis. $t_{1/2}$ of the bleached compartment (light green) = 19 ± 15, n = 5. Bar, 1 μm.

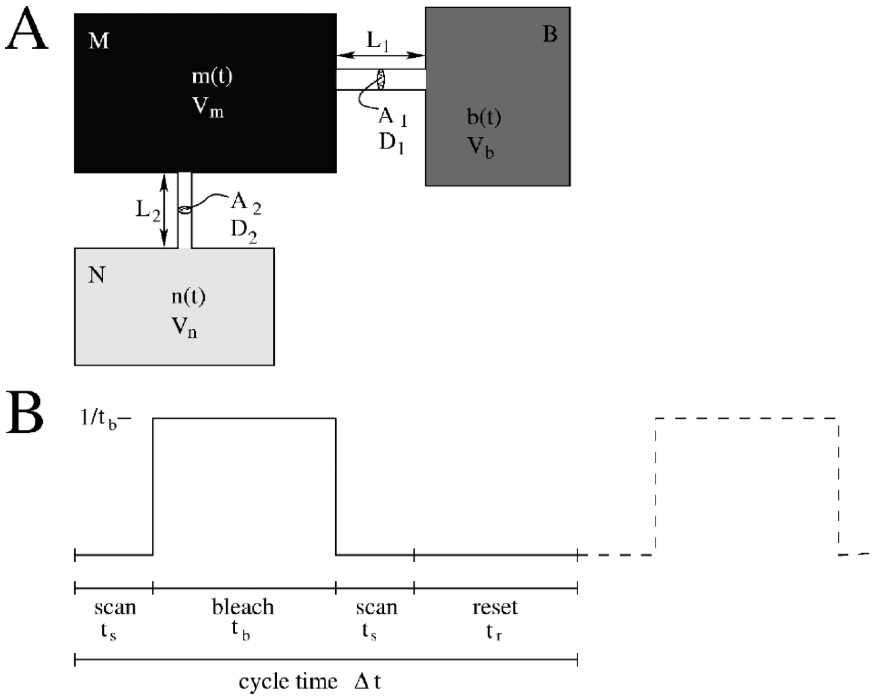

Figure S2. **System abstraction for modeling.** (A) The ER is modeled as three connected diffusion domains given by the mother cortical ER (M), mother perinuclear ER (N), and the ER of the bud (B). Each domain is attributed a volume V and a time-dependent fluorescence content: m(t), n(t), and b(t), respectively. Connections between the domains are characterized by their cross section area A, characteristic length L, and effective diffusion constant D. (B) FLIP cycle model. A FLIP experiment is modeled as repetitions of the cycle "scan–bleach–scan–reset." The height of the curve indicates the fluorescence drain applied to the bleached compartment.

for the membrane protein) A, its characteristic length L, and an effective molecular diffusion constant D. Because none of these transport parameters is known, they were combined into a single variable $\lambda = (DA)/L$, which has the physical units of volume/time and can be thought of as an effective "rate of transport."

The experimental bleaching and image acquisition cycle was modeled as depicted in Fig. S2 B. Each FLIP experiment consists of many repetitions of the cycle "scan–bleach–scan–reset," characterized by the respective time durations t_s, t_b, and t_r. The mathematical formulation of this "cycle function" is: $\beta(t) = [H(t - t_s) - H(t - t_s - t_b)]/t_b$, where $H(t)$ denotes the unit step function (Heaviside distribution). Conservation of mass in the whole system and Fick's Law of diffusion lead to the final model equations:

$$t(b(t)) = \lambda_1 \times (m(t)/V_m - b(t)/V_b) - (1 - \chi_m) \times v_b \times (b(t)/V_b) \times \beta(t - k$$

$$(m(t)) = \lambda_1 \times (b(t)/V_b - m(t)/V_m) + \lambda_2 \times (n(t)/V_n - m(t)/V_m) - \chi_m \times v_m \times (m(t)/V_m) \times \beta(t -$$

$$'dt(n(t)) = \lambda_2 \times (m(t)/V_m - n(t)/V_$$

$$\lambda_1 = D_1 \times A_1/L_1$$

$$\lambda_2 = D_2 \times A_2/L_2$$

$$(t) = [H(t - t_s) - H(t - t_s - t_b)]/$$

$\chi_m = 1$ if mother cortex is bleached and $\chi_m = 0$ if bud is bleached. Mathematically, they form a third order ordinary algebraic-differential equation model that was solved numerically using Matlab/Simulink (The Mathworks, Inc.) version 6.1.0.450 (R12.1) and a globally fourth order accurate Dormand-Prince (ode45) integration scheme with variable time step size adjusted to guarantee a relative tolerance (i.e., maximum error of the model solution) of 10^{-3}. The values v_b and v_m indicate the effective bleached volumes (i.e., the volume of the ER lumen [for GFP-HDEL] or the ER membrane area [for Sec61-GFP] within the bleached region) in the bud and the mother cortex, respectively. $k = 1, \ldots, k$ is the bleach cycle counter. Each bleach cycle has a duration of $\Delta t = 2 \times t_s + t_b + t_r$ (two scan, one bleach, and one reset period).

Quantitative values for the three unknown parameters λ_1, λ_2, and v (either v_b or v_m depending on which compartment was bleached) were obtained by fitting the solution of the above system of equations to experimental FLIP data, minimizing the total quadratic deviation between the model solution and the measurements at both pre- and postbleach points. This was done using Matlab (The Mathworks, Inc.) and a two-dimensional Nelder-Mead simplex minimization method. Minimization was done subject to the constraints $\lambda_1 > 0$, $\lambda_2 > 0$, and $v > 0$.

The initial value for λ_1 was set to 0.5, and the one for λ_2 to 5. Varying these values we found that for any initial λ_1 in the range of 0.005 to 1.0 and λ_2 between 0.1 and 10, the same fit (i.e., the same model parameter values) resulted. Even changing to an initial λ_1 of 1.0 while λ_2 was 0.1 did not change the outcome. If initial values outside above mentioned intervals were chosen, the model failed to fit the experimental data. This suggests that our model fit corresponds to the true (global) optimum of the fitting quality. The starting value for v (i.e., the effective bleached volume) was estimated from the first three data points of each experiment (fluorescence loss during the first bleach sequence) in order to increase the robustness of the minimization. The two volumes V_b and V_n were determined from the initial condition (steady state in both the model and the real system before the first bleaching pulse), and V_m was normalized to unity because we are only interested in relative comparisons and the FLIP data themselves were normalized before analysis too. 16 independent FLIP experiments were analyzed using this model. A sample outcome is shown in Fig. S3. The summarized results are in Table S1.

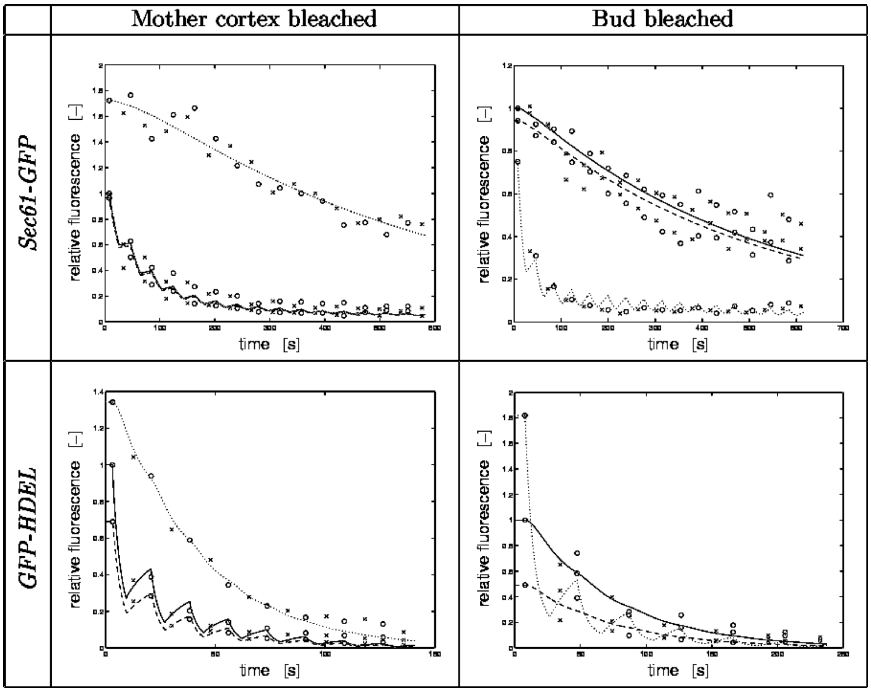

Figure S3. **Example of model fit to experimental FLIP data.** The solid lines correspond to the model prediction of the total fluorescence in the cortical ER of the mother cell, the dotted lines to the model prediction for the cortical ER of the bud, and the dashed lines to the perinuclear ER of the mother cell. Circles mark experimental postbleach scans and crosses mark the experimental prebleach scans. All data are processed and normalized as described in the main text.

Relative strength of the two connections: ER compartmentalization

No significant directionality could be seen. Diffusion from the mother to the bud seems equally fast as diffusion from the bud to the mother. Therefore, transport rates were considered independent of the direction and all values were averaged over the two bleach cases (mother bleached/bud bleached) using $n = 8$ experiments for each protein. For Sec61-GFP, we found $\lambda_{1,\text{Sec61-GFP}} = 0.00345 \pm 0.00162$ and $\lambda_{2,\text{Sec61-GFP}} = 14.623 \pm 6.487$ and for GFP-HDEL, $\lambda_{1,\text{GFP-HDEL}} = 0.0511 \pm 0.0240$ and $\lambda_{2,\text{GFP-HDEL}} = 13.664 \pm 4.718$, where the values are given as mean ± SD. We can state that for Sec61-GFP the connection between the cortical ER of the mother cell and its perinuclear ER is ~4,200 times stronger than the one between the cortical ER of the mother cell and the cortical ER of the bud. For GFP-HDEL, the ratio is ~270. Note that these ratios have nothing to do with the ratios of recovery half-times because the latter do neither account for the different volumes nor the fact that one protein diffuses in the luminal space whereas the other one is restricted to the membrane. Moreover, λ by definition not only contains the cross section but also the diffusion constant. Both a decreased ER cross section as well as an increased viscosity could thus be the reason for the observed transport barrier in the bud neck.

This compartmentalization effect would have for consequence that the mother cortex and the perinuclear ER would behave very much like a single compartment separated from the bud. To validate this prediction, we developed a second model with only two independent compartments, representing the mother cell (with perinuclear and cortical ER combined into the same compartment) and the bud. If it is true that the connection within the mother cell is orders of magnitude stronger than the one between mother and bud, the latter will dominate the dynamics of the whole system (transport rate–limiting connection) and a two-compartment model should approximate the experimental data about equally as well as the three-compartment model. The model was derived, implemented, and applied following the same steps and using the same methods as the above-described three-compartment model. Being a two-compartment model, the number of parameters is reduced by one to a single λ_1 (only one connection is modeled) and ν. We found that the mean model fit error per data point for the two-compartment model was 5.54 ± 1.73% and the maximum error we found in a single case was 9.0%. The three-compartment model had a mean error of 4.72 ± 1.36% and a maximum of 7.7%. The two-compartment model thus describes the data almost equally well and the two ER parts in the mother cell indeed seem to behave like a single compartment, as predicted by the λ values of the full three-compartment model. Note that the two-compartment model is only a control. The three-compartment model is closer to the biological reality and is needed to gain an idea of the relative strengths of the two connections (the two-compartment model only models one connection).

Together, these results provide evidence that the two ER compartments in the mother cell behave much like a single compartment, whereas the bud's ER is only weakly connected to it. This weakening of the connection seems to be more pronounced for the membrane-associated species than for the soluble one.

Membrane-associated versus soluble species: diffusion barrier in the membrane

From our model, we have numerical values for four different transport rates: soluble GFP-HDEL across the bud neck ($\lambda_{1,\text{GFP-HDEL}}$) and within the mother cell ($\lambda_{2,\text{GFP-HDEL}}$) as well as membrane-associated Sec61-GFP across the bud neck ($\lambda_{1,\text{Sec61-GFP}}$) and within the mother cell ($\lambda_{2,\text{Sec61-GFP}}$). We can now determine the ratio of the transport rates of the two species for each connection as: $\lambda_{1,\text{GFP-HDEL}}/\lambda_{1,\text{Sec61-GFP}} = 14.81$ and $\lambda_{2,\text{GFP-HDEL}}/\lambda_{2,\text{Sec61-GFP}} = 0.934$. Using the connection within the mother cell as a normalization standard, we find: $(\lambda_{1,\text{GFP-HDEL}}/\lambda_{1,\text{Sec61-GFP}})/(\lambda_{2,\text{GFP-HDEL}}/\lambda_{2,\text{Sec61-GFP}}) = 15.9$. This finding means that the soluble GFP-HDEL is exchanged ~16 times faster than the membrane-associated Sec61-GFP in the bud neck than it is

Table S1. **Summary of results of model fit**

	λ_1 mean ± SD	λ_2 mean ± SD	Mean fitting error (RMS)
Sec61-GFP mother bleached	0.00225 ± 0.00170	14.53 ± 6.74	4.451%
Sec61-GFP bud bleached	0.00435 ± 0.00090	14.71 ± 7.27	5.838%
GFP-HDEL mother bleached	0.06668 ± 0.01903	14.07 ± 3.89	3.652%
GFP-HDEL bud bleached	0.03042 ± 0.00790	13.12 ± 6.58	4.950%

The model fitting quality is quantified using the mean RMS error, which is the square root of the mean of all squared deviations between measured points and the model predictions at those points (i.e., the mean modeling error per data point). Because all data were normalized such that the first prebleach value of the mother cell's cortical ER was equal to 1, the RMS error can also be interpreted as a relative error in percent. Given our modelling errors of 4 to 6%, we consider the model fit to be good.

within the mother cell. In the model, the transport rate λ was defined as $\lambda = (DA)/L$. The effective diffusion coefficient of Sec61-GFP in the intra-mother connection is denoted by b. The one of GFP-HDEL is a_1 times larger, hence $a_1 b$. Similarly, the ratio of diffusion coefficients across the bud neck is termed a_2. For the standardized ratio, we thus find: $(\lambda_{1,\text{GFP-HDEL}}/\lambda_{1,\text{Sec61-GFP}})/(\lambda_{2,\text{GFP-HDEL}}/\lambda_{2,\text{Sec61-GFP}}) = (d_1 a_1)/(d_2 a_2)$, where d is the diameter of the respective connection. If the relative speed of diffusion of the two species across the bud neck is the same as in the mother cell, the connections in the bud neck would need to be 16 times thicker than the connections in the mother cell. From our EM data we know that this is not the case. The only explanation that is compatible with our observations is that the relative speed of diffusion is different in the two connections, meaning that the exchange of Sec61-GFP is slowed down 16-fold across the bud neck.

Altogether our calculations indicate that in no model Sec61-GFP and GFP-HDEL would be very likely to move together through the bud neck. In the case of vesicular-driven movement, one would have to postulate that incorporation of GFP-HDEL is favored over the packaging of Sec61-GFP. The molecular function of such a specific intra-ER traffic would be quite obscure. Alternatively, a diffusion barrier in the ER membrane would explain why GFP-HDEL moves more rapidly through the bud neck than Sec61-GFP. This model is in very good agreement with our morphological data that suggest the presence of a cylinder of smooth ER linking the mother and bud ER.

Shape of mother–bud connection: exclusion of vesicular transport

Using the definition of λ_1 and some basic geometric considerations allows rough statements about the geometric shape of the mother–bud ER connection and about whether vesicular transport could also explain the measurements. We consider three cases: (1) mother and bud ER are connected with a set of tubules, (2) they are connected by a cylindrical ring of smooth ER, or (3) they are not directly connected, but vesicular transport takes place between them.

First, for tubular connections with N tubules of mean radius r, the total cross section of the connection is given by $N \times \pi \times r^2$. This is the area through which GFP-HDEL diffuses. The total membrane cross-cut of the connection is $2 \times N \times \pi \times r$. This is the "area" through which Sec61-GFP moves. Furthermore, we let the diffusion constant of GFP-HDEL be a_1 times larger than the one of Sec61-GFP. The ratio of transport rates of the two species then becomes: $\lambda_{1,\text{GFP-HDEL}}/\lambda_{1,\text{Sec61-GFP}} = (a_1/2) \times r$.

Second, for a continuous cylindrical connection (as suggested by the EM pictures in Fig. 4) with mean outer radius R and mean inner radius r, we have a total cross section of $(R^2 - r^2) \times \pi$ and a total surface line of $2 \times \pi \times (R + r)$. The ratio of transport rates hence becomes $\lambda_{1,\text{GFP-HDEL}}/\lambda_{1,\text{Sec61-GFP}} = (a/2) \times (R - r) = (a_1/2) \times h$ with the ER lumen thickness h (thickness of the cylinder wall).

Third, for vesicular transport, we recall that λ_1 is "volume per time." If we assume a mean of N spherical vesicles to be involved in the transport at any time and a mean vesicle travel time of τ seconds, the volume (GFP-HDEL) transport rate is $N \times (4 \times \pi/3) \times r^3/\tau$ and the surface area (Sec61-GFP) transport rate is $N \times 4 \times \pi \times r^2/\tau$. The ratio of transport rates thus becomes: $\lambda_{1,\text{GFP-HDEL}}/\lambda_{1,\text{Sec61-GFP}} = r/3$, provided that luminal and membrane proteins are equally well packaged into vesicles.

From fitting the model to experimental FLIP data, we know that $\lambda_{1,\text{GFP-HDEL}}/\lambda_{1,\text{Sec61-GFP}}$ is roughly 15. Assuming unhindered diffusion within the mother cell, the ratio of diffusion constants is about $a_2 = 40$ (GFP-KDEL: 10–30 $\mu m^2/s$ [Dayel et al., 1999]; Sec61: typical value for membrane proteins: 0.5 $\mu m^2/s$ [Lippincott-Schwartz et al., 2001]). Using the result $a_1 = 16a_2$ from the previous section gives a relative speed of diffusion of $a_1 = 640$ across the bud neck. This enables us to estimate the order of magnitude of some geometric properties. For the first case, we get a mean tubule radius of ~0.05 μm and for the second case, a cylinder thickness of also ~0.05 μm. For the third case, we find that the mean vesicle radius for vesicular transport would have to be ~45 μm. Given the simplifications in our model (we have neglected the precise geometry and the fact that D is only the effective diffusion constant and not the molecular one) and the uncertainties in the literature values of the diffusion constants, these numbers are to be considered rough estimates and could well be a factor of 10 wrong. Still, the 50-nm cylinder thickness in the second case is in nice agreement with our electron micrographs. In light of these numbers, vesicular transport is entirely unrealistic. These calculations are consistent with our experimental results and vesicular transport through the bud neck can be ruled out.

Model validation, accuracy, and limitations

Our model is limited by the assumptions made in the process of deriving it. It is important to stress that the model (and thus all of its conclusions) is only valid if the transport between mother and bud is a process of passive diffusion. The accuracy with which the model is able to approximate our experimental data, together with the observations described in the main text (see Fig. 4; sodium azide), however, strongly suggest that this is actually the case. Furthermore, we have assumed that there is no direct connection between the perinuclear ER in the mother and the cortical ER of the bud and that the total fluorescent mass in the whole ER body is conserved for the duration of the experiment; i.e., no net protein export/import from/to the ER. The latter assumption was verified in experiments on cells expressing Sec61-GFP and treated with sodium azide (Fig. 4), as the dynamics of diffusion are not altered in the absence of energy. The former assumption was tested using another variation of our model. It had the connection between the mother cortex and the bud cortex replaced by one between the perinuclear ER and the bud cortex. This modified model was completely unable to fit the data in the cases where the bud was bleached. This is evidence that there is no direct connection between the perinuclear ER and the bud cortex. Another important limitation of the current method is the fact that all data as well as the model were normalized by the first prebleach value of the mother cortex. This makes sense to circumvent difficulties otherwise caused by (unknown) absolute length scales in the experiments. Without normalization, at least one of the three ER compartment lumen volumes (and surface areas for the membrane protein) would need to be measured in absolute numbers to calibrate the model. Normalization eliminates this need but also prevents any conclusions based on absolute values of transport rates or diffusion constants. The model transport rates λ are in fact dimensionless rather than giving values in micrometers cubed per second. Only relative comparisons are admissible using such a model.

As far as model accuracy is concerned, we notice that the mean RMS model fitting error (i.e., the mean error per data point) is 4.72 ± 1.36% and the maximum error we found was 7.7%, corresponding to a maximum modeling uncertainty of <10%. This is of the same order of magnitude as the experimental uncertainty and thus no significant reservation can be made. A more limiting aspect is that λ_2 is hardly identifiable from the data if the bud is bleached. This is due to the fact that the bud and the perinuclear ER are only indirectly connected and changes in the transport rate "perinuclear ER → cortical mother ER" have only minor influences on the fluorescence evolution in the bud. We empirically observed that changing λ_2 by a factor of two only changes the other parameters (including the fitting error) at the third position after the decimal point. Any difference of less than a factor of 10 in λ_2 must therefore be considered insignificant, given the numerical tolerance of 10^{-3} used in solving the model. This insensitivity to λ_2 does not however affect any conclusions based on λ_1, as the model is highly sensitive there.

References

Dayel, M.J., E.F. Hom, and A.S. Verkman. 1999. Diffusion of green fluorescent protein in the aqueous-phase lumen of endoplasmic reticulum. *Biophys. J.* 76:2843–2851.

Lippincott-Schwartz, J., E. Snapp, and A. Kenworthy. 2001. Studying protein dynamics in living cells. *Nat. Rev. Mol. Cell Biol.* 2:444–456.